Kinetics and Mechanism of Conformational Changes in a G-Quadruplex of Thrombin-Binding Aptamer Induced by Pb2+

ARTICLE *in* THE JOURNAL OF PHYSICAL CHEMISTRY B · SEPTEMBER 2011

Impact Factor: 3.3 · DOI: 10.1021/jp2074489 · Source: PubMed

7 AUTHORS, INCLUDING:

Liu Wei
University of Science and Technology of Ch…
6 PUBLICATIONS **71** CITATIONS
SEE PROFILE

Bin Zheng
Hefei Normal University
16 PUBLICATIONS **165** CITATIONS
SEE PROFILE

Haojun Liang
University of Science and Technology of Ch…
152 PUBLICATIONS **2,247** CITATIONS
SEE PROFILE

View Online / Journal Homepage / Table of Contents for this issue
Dynamic Article Links

Soft Matter

Cite this: *Soft Matter*, 2012, **8**, 3017

www.rsc.org/softmatter

PAPER

G-quadruplex formation and sequence effect on the assembly of G-rich oligonucleotides induced by Pb^{2+} ions

Wei Liu,[abc] Bin Zheng,[abc] Sheng Cheng,[abc] Yan Fu,[d] Wei Li,[*e] Tai-Chu Lau[*bc] and Haojun Liang[*ab]

Received 11th April 2012, Accepted 16th May 2012
DOI: 10.1039/c2sm25839k

The lead-induced folding into G-quadruplex structures for three guanine-rich oligonucleotides, two model human telomeric oligomers (HTG/T2) and thrombin-binding aptamer (TBA), was characterized by equilibrium titrations, rapid mixing techniques and stopped-flow kinetics. The analysis of optical titration data reveals that the saturated Pb^{2+}–DNA binding stoichiometries are 1 : 1, 2 : 1 and 3 : 1 for TBA, HTG and T2, respectively. Thermal denaturation experiments were performed to determine the structural stability. The overall results are consistent with the higher stability of T2 that contains four G-quartets, as opposed to HTG and TBA that have only three and two quartets, respectively. We also present kinetic studies of the formation of G-quadruplexes of G-rich DNA induced by Pb^{2+} ions. The binding of Pb^{2+} ions to G-DNA is a complex multiple pathway process, which is affected by the sequence of the G-DNA. The studies show that the connecting loops of the DNA play an important role in modulating the structures.

Introduction

Guanine-rich oligonucleotides can be assembled into four-stranded DNA structures that are generally stabilized by certain cations.[1–5] Interest has been stimulated by the possible roles of G-quadruplex structures as lead molecules in drug design[6,7] and as structural motifs potentially adopted by telomere,[8] regulators in immunoglobin switching,[9,10] centromere DNA, and other biological systems,[11,12] although there is little direct evidence of G-quadruplex formation and function *in vivo*. G-Quadruplexes are also being considered as possible drug targets for telomerase inhibition and other roles.[13–16] In addition, the polymorphic nature of the G-quadruplexes is promising for nanotechnology applications.[17] Thus, regulating the structural polymorphism of the G-quadruplexes can lead to the development of a novel methodology that can be used to investigate biological phenomena, functional molecules, and nanomaterials related to G-quadruplexes.

G-Quadruplexes are highly polymorphic with respect to several structural features, including strand orientation (*i.e.*, parallel *vs.* antiparallel) and strand number (*e.g.*, uni-, bi-, and tetramolecular). G-Quadruplex topologies are determined by several factors, including the type of cations present,[18] the composition of the loops[19–21] and the number of stacked G-tetrads.[22] Unlike other known DNA structures, G-quartets interact directly with dehydrated cations *via* inner-sphere coordination.[23] The formation, stability, and structural details of G-quadruplexes are consequently dependent on the nature and concentrations of the cations. Owing to their physiological importance, Na^+ and K^+ ions are the most extensively characterized with respect to their ability to stabilize G-quadruplex structures. Ions such as K^+ and NH_4^+ are too large to coordinate in the plane of a G-quartet, whereas Na^+ is small enough to be coordinated within the plane of a G-quartet. Hud and co-workers reported that $[d(G_4T_4G_4)_2]$ coordinates three NH_4^+ ions, one in each of the two symmetry related sites and one on the axis of symmetry of the dimeric molecule.[24,25] A number of divalent cations also promote G-quadruplex formation. Sr^{2+} ions were observed to be coordinated between every other pair of stacked G-quartets with the eight carbonyl oxygen atoms of the adjacent G-quartets in a bipyramidal-antiprism geometry.[26–29] The Pb^{2+} ion binds more effectively than K^+ and induces a monomolecular fold that is similar to the structure formed in the presence of K^+.[30–32] Davis and co-workers showed that lipophilic G-analogues in the presence of Pb^{2+} associate to form quadruplex-like structures in organic solvents.[30] These observations indicate that the Pb^{2+} ion, compared to the K^+ ion, induces

[a]*CAS Key Laboratory of Soft Matter Chemistry, Hefei National Laboratory for Physical Sciences at the Microscale, University of Science and Technology of China, Hefei, Anhui 230026, P. R. China. E-mail: hjliang@ustc.edu.cn; Tel: +86-551-3607824*
[b]*Advanced Laboratory for Environmental Research and Technology (ALERT), Joint Advanced Research Center, USTC-CityU, Suzhou, Jiangsu 215124, P. R. China. E-mail: bhtclau@cityu.edu.hk*
[c]*Department of Biology and Chemistry, City University of Hong Kong, Tat Chee Avenue, Kowloon, Hong Kong, P. R. China*
[d]*Key Laboratory of Systems Bioengineering, Ministry of Education, School of Chemical Engineering and Technology, Tianjin University, Tianjin 300072, P. R. China*
[e]*Key Laboratory for Green Chemical Technology, Ministry of Education, School of Chemical Engineering and Technology, Tianjin University, Tianjin 300072, P. R. China. E-mail: liwei@tju.ed.cn*

a more stable and compact structure, which is evident from the results of comparisons of cation–O6 bond lengths, O6–O6 diagonal distances, and inter-quartet separation.[30–32]

Quadruplex conformations in the presence of Pb^{2+} are of particular interest because the genotoxicity of Pb^{2+} ions may arise partially from its strong binding to a quadruplex formation in the genome. This condition is especially observed in the promoter regions, where quadruplexes can serve as transcription switches. If Pb^{2+} can displace K^+ from a quadruplex, but not *vice versa*, then the switching function of the structure may be hindered, providing an explanation for the genotoxicity of Pb^{2+} ions. Furthermore, Pb^{2+} ions induce the assembly of G-rich DNA into G-quadruplexes at micromolar concentrations. Other ions, like K^+ and Sr^{2+} also have stabilizing effects on G-tetrads, but they have to be in much higher concentrations than the effective concentration of Pb^{2+}.

Although several reports have focused on the cation-induced folding of G-rich DNA, the kinetics of the formation of monomolecular G-quadruplexes has not been extensively investigated.[33] Kinetic studies can provide insights into the possible mechanism of G-rich DNA folding, as well as the intermediates involved in the process.[34,35] In the present work, we examined the formation of G-quadruplexes of three models of G-rich DNA induced by Pb^{2+}. A thrombin-binding aptamer (TBA), $d(G_2T_2G_2TGTG_2T_2G_2)$, can form a G-quadruplex structure, where two G-quartets are interconnected through the lateral TT and TGT loops in an antiparallel conformation; and it possesses a high affinity for thrombin.[36–39] Human telomeric DNA (HTG), $d[AG_3(T_2AG_3)_3]$, forms a basket structure characterized by antiparallel, two lateral loops and one diagonal loop.[40] Another telomere-related sequence (T2), $(G_4T_2G_4T_2G_4T_2G_4)$, folds into a G-quadruplex structure with antiparallel strand orientations.[26]

Experimental section

Chemicals and reagents

The G-rich oligonucleotide, 2-(*N*-morpholino)ethanesulfonic acid (MES) and tris(hydroxymethyl)aminomethane (tris) were purchased from Shanghai Sangon Biological Engineering Technology and Services Co., Ltd. (China). All nitrate salts were of analytical grade and used without further purification. The oligomer samples were dissolved in a buffer solution consisting of 10 mM MES–Tris at pH 6.1. The oligomer solutions were then heated in a dry bath to 95 °C (ABSON, U.S.), equilibrated for 15 min at this temperature and then slowly cooled to room temperature. The concentrations of single-strand DNA were determined at 260 nm using a UV-vis spectrophotometer, using the following molar extinction coefficients at 260 nm of 146.0 mM^{-1} cm^{-1}, 228.5 mM^{-1} cm^{-1}, and 236.2 mM^{-1} cm^{-1} for TBA, HTG and T2, respectively.[41]

Circular dichroism (CD)

CD spectra were obtained using a JASCO J-810 spectropolarimeter at 25 °C, which was maintained by a Julabo temperature controller. The final oligomer concentrations were in the range 15–25 μM. Each measurement was recorded from 220 to 350 nm at a scan rate of 100 nm min^{-1} using a sealed 1 mm path-length quartz cuvette. The spectra were collected with a response time of 0.1 s and data intervals of 0.2 nm. The final spectra were the averages of three measurements. The scan of the buffer alone under the same conditions was used as the blank, and was subtracted from the average scan for each sample. The cell holding chamber was flushed with a constant stream of dry nitrogen gas to avoid water condensation on the cell exterior.

UV-Vis absorption titration experiments

The extent of the G-rich DNA folding was evaluated by measuring UV absorbance changes at 303 nm as a function of the concentration of added $Pb(NO_3)_2$. These experiments are required prior to the kinetic experiments, not only to establish the expected changes in absorption, but also to determine the minimum concentration of $Pb(NO_3)_2$ necessary for inducing complete folding. UV absorption spectra were measured at 1 nm intervals from 220 to 350 nm using a Shimadzu 1800 spectrophotometer (Shimadzu, Japan) equipped with a digital circulating water bath maintained at 25 °C. Equal volumes of $Pb(NO_3)_2$ and oligomer in the same buffer were mixed in a sealed tandem cuvette with a path length of 10 mm. The oligomer concentration before and after mixing was 5.0 and 2.5 μM, respectively. After each addition of $Pb(NO_3)_2$, the difference spectra $\Delta A^{\lambda} = A^{\lambda}_{U} - A^{\lambda}_{F}$ were obtained by subtracting the absorption spectrum from the spectrum of the fully unfolded oligonucleotide. Titration data ($\Delta\varepsilon$), were then plotted as a function of the concentration of $Pb(NO_3)_2$.

Thermal denaturation experiments

Nucleic acid structures are sensitive to temperature. Hence, UV melting profiles can be used to determine the melting temperature (T_m) of the cation-induced G-quadruplexes and the temperature range in which the complexes are stable. In a typical experiment, the melting curve was obtained by monitoring the UV absorbance at 303 nm as a function of temperature using a sealed 10 mm path-length quartz cell. The samples were first allowed to stand at 15 °C for 5 min and then heated to 95 °C at a heating rate of 0.2 °C min^{-1}. The T_m values of the complexes were calculated by fitting the experimental curves with a Sigma plot,[42] where T_m is the midpoint temperature of the order–disorder transition of the complex.

Stopped-flow kinetic experiments

The kinetic experiments for Pb^{2+}-induced oligomer folding were performed by monitoring absorbance changes using an Applied Photophysics SX-20 stopped-flow spectrophotometer. Before measurement, the oligomer samples were thermally treated as described above and incubated at the desired temperature for several minutes. Absorption spectra were obtained from 250 to 350 nm with 4000 time points. We discarded the data points collected at wavelengths <270 nm and the data before dead time prior to analysis to avoid a low signal-to-noise ratio at the shorter wavelengths and the dead-time points.[43] A circulating water bath was used to maintain a constant reaction temperature. The kinetic experiments were performed under pseudo-first-order conditions with the concentrations of $Pb(NO_3)_2$ at least in

10-fold excess of those of the oligomers. At least five successive mixing experiments were performed, and the results were averaged for analysis. Control experiments, consisting of mixing oligomers in cation-free buffer, were also performed. Single-wavelength progress curves were analyzed by nonlinear least-squares, using single or multiple exponentials (Eq. (1)) to determine the relaxation times for the formation of G-quadruplexes:

$$A_{t,\lambda} = A_{1,\lambda} \times \exp(-t/\tau_1) + A_{2,\lambda} \times \exp(-t/\tau_2) + A_{3,\lambda} \times \exp(-t/\tau_3) + A_{0,\lambda} \quad (1)$$

where $A_{t,\lambda}$ is the absorbance at time t, $A_{0,\lambda}$ is the initial absorbance, $A_{1,\lambda}$, $A_{2,\lambda}$ and $A_{3,\lambda}$ are the amplitude factors for the first, second, and third exponentials at wavelength λ, respectively. τ_1, τ_2, and τ_3 are the relaxation times, respectively.

Results and discussion

Circular dichroism spectra

CD spectra of the G-rich DNA were collected in the presence and absence of metal ions to obtain an indication of metal ion induced structure formation (Fig. 1). The addition of 0.5 mM $NaNO_3$ has little effect on the structures of the oligomers. On the other hand, the spectra of the G-rich DNA show a hyperchromic shift near 295 or 312 nm in the presence of 0.5 mM KNO_3 or $Pb(NO_3)_2$, respectively, indicating the formation of G-quadruplex structures. In the presence of $Pb(NO_3)_2$, the intensity of the maximum is much higher than that of $NaNO_3$ or KNO_3, which may be related to the structural stability of the G-quadruplexes. The absorption intensity of the Pb^{2+}-induced G-quadruplex of HTG is up to 15 times higher than those of the K^+-induced ones, which may be attributed to the extremely high affinity of HTG to the Pb^{2+} ions and the compact G-quadruplex structure that resulted from the coordination of HTG with Pb^{2+}. The spectra of the cation-induced G-quadruplex of T2 are very different from those of the other G-rich DNA. The locations of the maxima in the spectra of T2 are also at 295 or 312 nm in the presence of KNO_3 or $Pb(NO_3)_2$, respectively, whereas the minimum has shifted. Moreover, the absorption intensity in the spectra of T2 is much lower than that of TBA and HTG. These results may be attributed to the limited lengths of the loops and the generation of a much less compact structure of T2. The overall results reveal that the structures of cation-induced G-quadruplexes are greatly influenced by the sequences and the loop lengths of the G-rich DNA.

Folding equilibrium titration

Previous studies have shown that the UV absorption spectrum of the Pb^{2+}-driven folded G-quadruplex exhibits an absorption maximum at ~303 nm, which is distinctly different from those of the unfolded oligonucleotides.[44,45] Oligomers (TBA, HTG and T2) were titrated with micromolar concentrations of $Pb(NO_3)_2$ at 25 °C to monitor the absorbance change and to determine the cation binding number. The absorbance change at 303 nm was recorded as a function of the mole ratio of cation to oligomers, and the results are shown in Fig. 2. The spectra in the left panels of Fig. 2 indicate that the Pb^{2+}-induced folding of G-rich DNA is accompanied by relatively

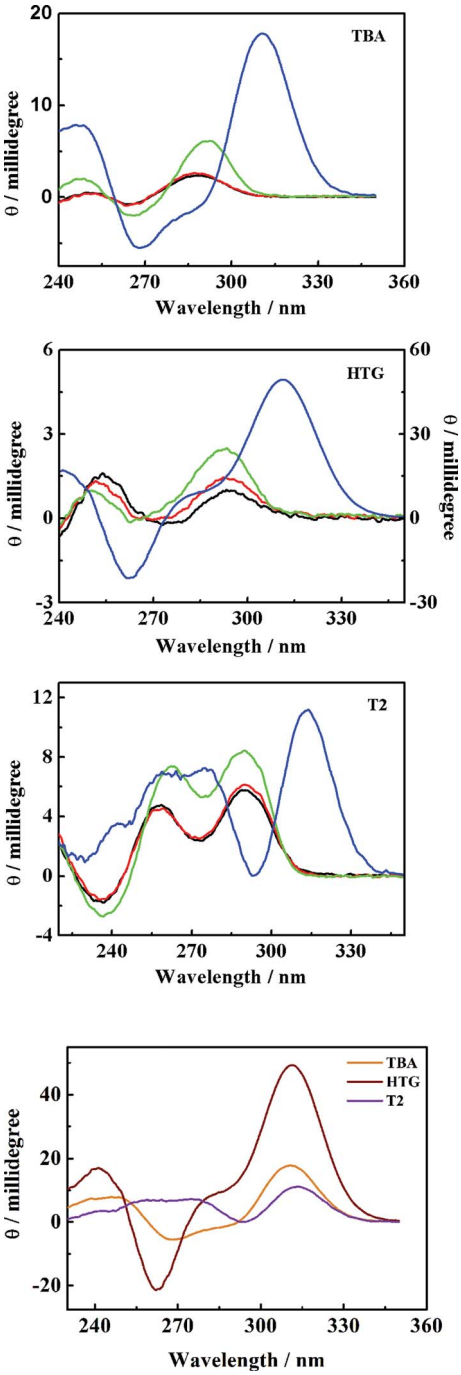

Fig. 1 CD spectra of cation-induced G-quadruplexes of G-rich DNA in the absence (black) or presence of various cations (Na^+ red, K^+ green and Pb^{2+} blue) in buffer solution (10 mM MES–Tris, pH 6.1) at 25 °C. The concentrations of the oligonucleotides were 25 μM after mixing.

smaller absorbance changes between 235 and 285 nm but larger absorbance changes between 285 and 340 nm, with maxima and minima at ~245/~275 and ~303 nm, respectively. As the concentration of Pb^{2+} increases, the characteristic peak of the G-quadruplexes decreases. Plots in the right panel of Fig. 2 indicate that the [Pb^{2+}]/[DNA] mole ratios for TBA and HTG are 1 and 2, respectively. These values are consistent with the proposed G-quadruplex structures of TBA and HTG with two and three G-quartets, respectively. Experimental results of T2

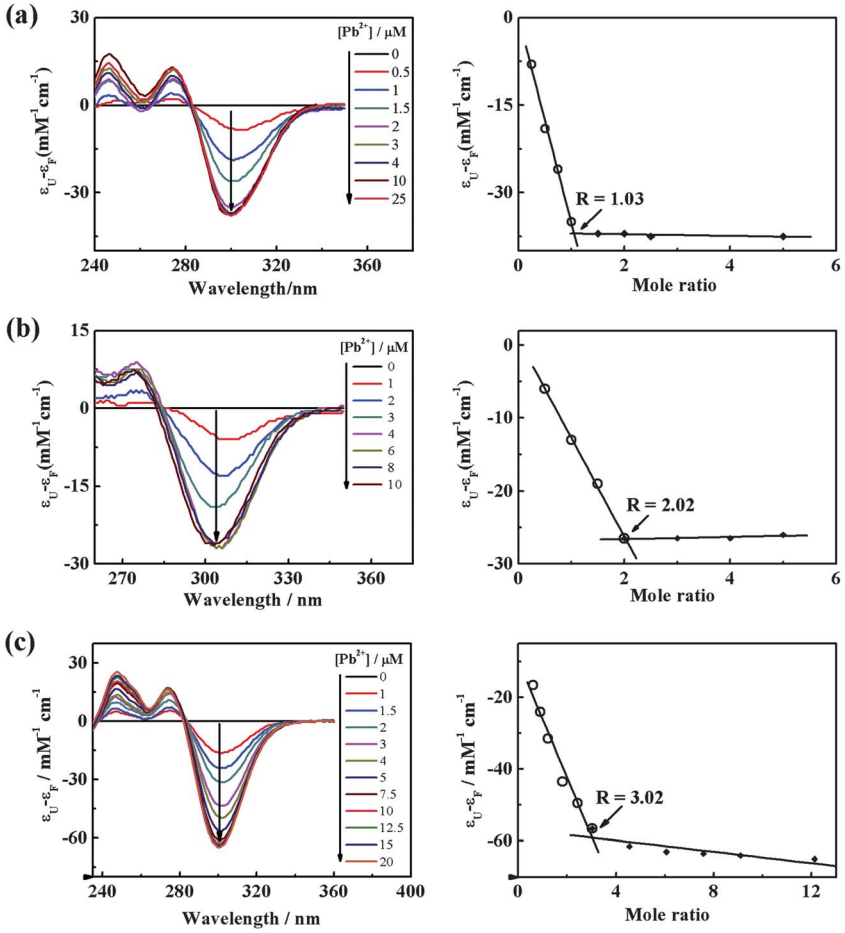

Fig. 2 Spectrophotometric titrations of G-rich DNA (2.5 μM) with $Pb(NO_3)_2$. (a) TBA, (b) HTG, (c) T2. Images in the left panels indicate spectral changes in the titration process. Arrows indicate a decreasing absorbance change upon successive additions of cations. Final cation concentrations after mixing are shown in the right panel. Right panels show plots of absorbance changes at 303 nm against the mole ratio of $Pb(NO_3)_2$ to oligomers. The temperature was maintained at 25 °C.

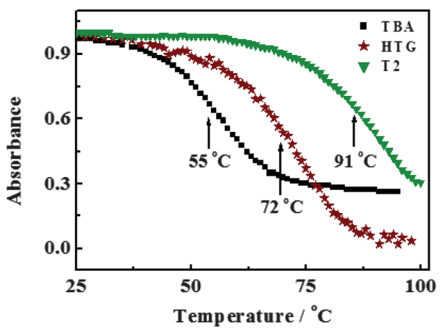

Fig. 3 Denaturation profiles at 303 nm for G-rich DNA (2.5 μM) induced by Pb^{2+} ions in buffer solution (10 mM MES–Tris, pH 6.1).

show that the absorbance of T2 decreases slightly as the mole ratio increases, and that at least three Pb^{2+} ions are needed for the formation of a G-quadruplex. The G-quadruplex of T2 is proposed to have four G-quartets, consistent with the literature.[46] The Pb^{2+}-induced G-quadruplex of T2 has a loose structure because of the relatively short loops of the T2 strand. Hence, more cations are needed to stabilize this structure. The titration data are consistent with the proposed sandwich structures, in which Pb^{2+} ions bind between the adjacent G-quartets.[34,35]

Thermal denaturation profiles

UV melting experiments were performed to examine the stability of the cation-induced G-quadruplexes. The unfolding profiles of the cation-induced G-quadruplexes were monitored at 303 nm, which is the characteristic peak in the spectra of the G-quadruplexes (Fig. 3). All the curves indicate monophasic transitions with different cooperativities. Broad and sharper transitions are observed, depending on the compactness of the generated structure. The T_m values of the Pb^{2+}-induced G-quadruplexes of the G-rich oligomers are 55, 72 and 91 °C for TBA, HTG, and T2, respectively. These parameters have a close relationship with the number of the G-quartets in their structures. The higher T_m for the Pb^{2+}–T2 complex is consistent with the four G-quartets. However, the wide temperature range shown in the spectrum of T2 indicates that the complex has a loose structure. The transitions of the Pb^{2+}-induced G-quadruplexes of TBA or HTG are sharper, consistent with the proposed compact structures. These

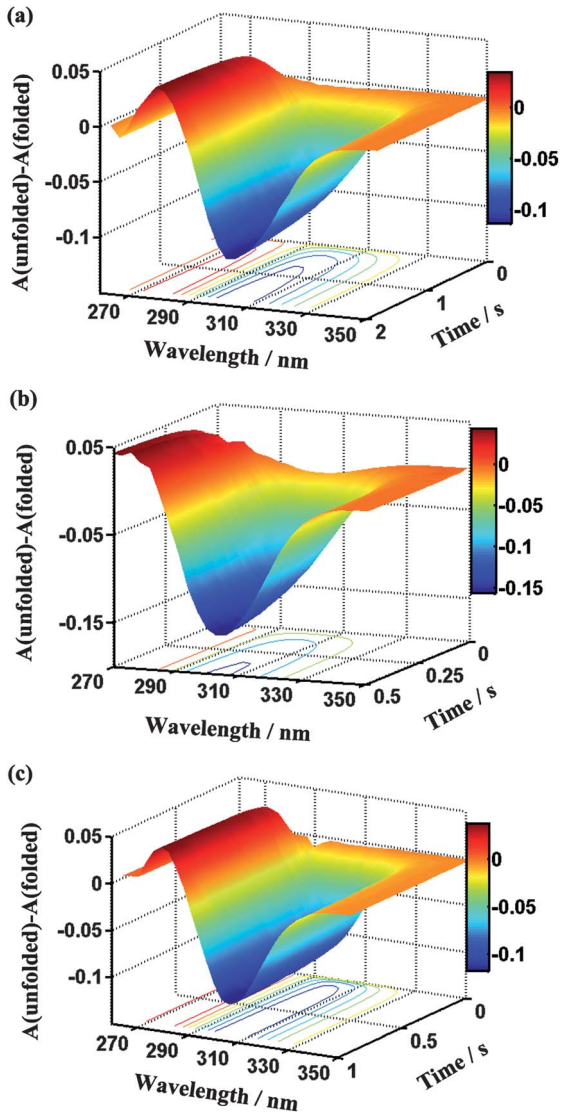

Fig. 4 Representative 3D plots of the wavelength and time dependence of the spectrophotometric changes accompanying Pb^{2+}-induced folding of the G-rich oligomers ((a) TBA, (b) HTG, (c) T2). The G-rich DNA (5.0 μM) were mixed with $Pb(NO_3)_2$ (20 μM) in buffer solution (10 mM MES–Tris, pH 6.1). The reaction temperature was kept at 25 °C.

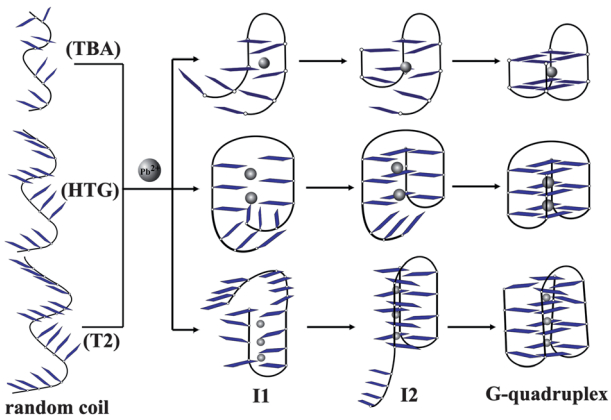

Fig. 6 The proposed mechanisms for the formation of the G-quadruplexes of G-rich DNA induced by Pb^{2+} ions. I1 and I2 indicate intermediate 1 and intermediate 2, respectively. Rectangles represent the G bases.

results show that the structures of the complexes are greatly influenced by the number of G-quartets and loops of the G-quadruplexes.

Stopped-flow measurements

Spectrophotometric changes of the Pb^{2+}-induced G-quadruplex of G-rich DNA. To our knowledge, there are few studies on the application of repetitive scanning in UV spectra to elucidate the mechanism of G-quadruplex formation.[33] Since the time scale of the folding of the G-quadruplex is very short, we made use of the rapid stopped-flow mixing technique to monitor the spectrophotometric changes that accompany Pb^{2+}-driven G-quadruplex formation. Fig. 4 shows the spectrophotometric changes in the UV difference spectra $\Delta A^{\lambda} = A^{\lambda}_{U} - A^{\lambda}_{F}$ for the folding process of ~2.5 μM oligonucleotides induced by 10 μM $Pb(NO_3)_2$. Data points were collected at wavelengths between 270 and 350 nm to avoid a high noise-to-signal ratio. The Pb^{2+}-induced folding of TBA, HTG, and T2 was characterized by rapid mixing at intervals of 0.04, 0.01, and 0.02 s, and the folding processes were completed within 2, 0.5, and 1 s, respectively. The growth of a negative peak at approximately 303 nm indicates the formation of a Pb^{2+}-induced G-quadruplex.

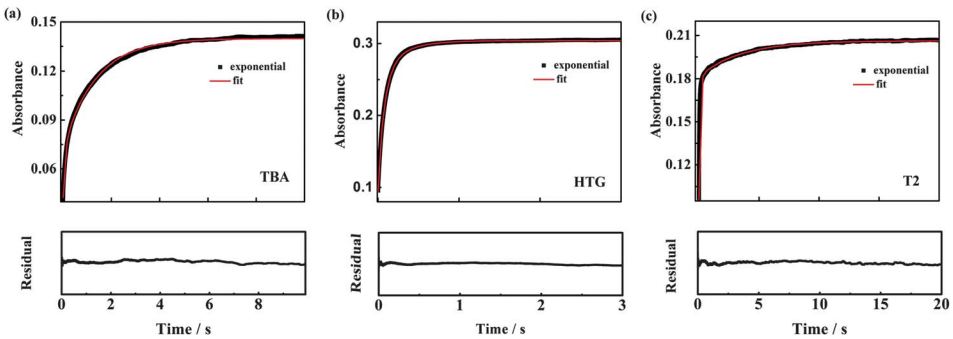

Fig. 5 Representative absorbance (303 nm) *versus* the time trace of the folding of G-rich DNA (2.5 μM) induced by $Pb(NO_3)_2$ (0.2 mM). All measurements were performed in a buffer containing 10 mM MES–Tris (pH 6.1) at 25 °C. The red line shows the nonlinear least-squares fit of the dataset to the three exponentials. The residual plot indicates the deviation of the experimental and fitted absorbance changes.

Time-tracing curves of the Pb^{2+}-induced folding of the G-rich oligonucleotides into G-quadruplexes. The time-tracing curves of the folding process were obtained by monitoring absorbance changes at 303 nm, the maximum signal in the spectra of the Pb^{2+}-induced G-quadruplexes. The experimental and calculated profiles, as well as the residual plots, are shown in Fig. 5. In the presence of at least a 10-fold excess of $Pb(NO_3)_2$, the time-tracing curves are best fit to three sequential first-order processes (modeling the U → I1 → I2 → F reaction pathway); the residual plots show that the three exponential models fit the experimental curves very well. On the other hand, fitting to single or double exponential rate expressions results in larger systematic deviations between the fitted and experimental curves. A set of five plots were analyzed, and the optimal relaxation times (τ) were obtained. The relaxation times for the folding process in the TBA model were $\tau_1 = 0.006 \pm 0.001$ s, $\tau_2 = 0.15 \pm 0.01$ s and $\tau_3 = 1.54 \pm 0.01$ s for the three steps. τ_1 is similar to the previous data obtained from the CD stopped-flow measurements.[34] The relaxation times of the folding of HTG were determined to be $\tau_1 = 0.009 \pm 0.001$ s, $\tau_2 = 0.079 \pm 0.001$ s and $\tau_3 = 0.29 \pm 0.01$ s. The relaxation times are quite short, indicating the high affinity of HTG for Pb^{2+} ions. The relaxation times for the T2 model were relatively longer, $\tau_1 = 0.024 \pm 0.001$ s, $\tau_2 = 0.14 \pm 0.01$ s and $\tau_3 = 3.56 \pm 0.03$ s. The Pb^{2+} ions may require a longer time to assemble the T2 strand into the G-quadruplex structure with four G-quartets because of the shorter loops.

The mechanism of the formation of G-quadruplexes. Based on the kinetic and equilibrium studies, the mechanisms for the formation of the G-quadruplexes of G-rich DNA are proposed, as shown in Fig. 6. In these mechanisms, the Pb^{2+}-induced quadruplex folding of G-rich DNA involves three steps. First, Pb^{2+} ions bind to the strand, which may result in the partial folding of the oligomer. Second, the strand is modulated by Pb^{2+} ions to give a metastable structure. Lastly, the structure rearranges to form the final sandwich structures of the G-quadruplexes. We infer that the proposed sandwich structures of the Pb^{2+}-induced G-quadruplexes are the most reasonable, based on our results and data from the literature, although different G-quadruplex structures have been reported.[27] The connecting loops of the G-quadruplexes, as mentioned in a previous study, may play important roles in the formation of these structures.[47,48] The differences observed in the kinetics of G-quadruplex formation may be caused by the sequence and the loop length effects.

Conclusions

A detailed knowledge of the mechanism of intramolecular G-quadruplex formation is of prime importance for the design and fabrication of quadruplex-based nanostructures or therapeutic agents. We reported in this study the kinetics and the mechanism of the formation of G-quadruplexes of G-rich DNA induced by Pb^{2+} ions. Sequence effects on the assembly of G-quadruplexes have also been investigated. CD and UV measurements illustrate the characteristic spectra of the Pb^{2+}-induced G-quadruplexes. Equilibrium titration demonstrates that the Pb^{2+} ions assemble TBA, HTG, and T2 into G-quadruplexes with two, three and four G-quartets, respectively, with Pb^{2+} ions coordinating between the adjacent quartets. UV melting experiments indicate that the Pb^{2+}-induced G-quadruplexes of TBA and HTG are compact, whereas T2 is induced to a relatively loose G-quadruplex structure, resulting in a broad transition in melting studies. Kinetic studies show that the Pb^{2+}-induced folding of G-rich DNA into G-quadruplexes probably proceeds through a three-step pathway with two intermediates. From these studies, it can also be found that the sequence of the G-rich DNA greatly influences the formation of the G-quadruplexes. We believe that the present findings represent a significant step towards the understanding of the complexity of ion binding as well as the dynamics in G-quadruplex structures and nucleic acids in general.

Acknowledgements

This work was supported by the National Natural Science Foundation of China (grant nos. 20934004 and 91127046); NBRPC (grant nos. 2012CB821500 and 2010CB934500) and the "Bairen" fund of CAS.

References

1 M. K. Raghuraman and T. R. Cech, *Nucleic Acids Res.*, 1990, **18**, 4543–4551.
2 S. Basu, A. A. Szewczak, M. Cocco and S. A. Strobel, *J. Am. Chem. Soc.*, 2000, **122**, 3240–3241.
3 M. A. Keniry, *Biopolymers*, 2000, **56**, 123–146.
4 B. H. Ozer, B. Smarsly, M. Antonietti and C. F. J. Faul, *Soft Matter*, 2006, **2**, 329–336.
5 G. N. Parkinson, *Fundamentals of quadruplex structures*, RSC Publishing, Cambridge, UK, 2006, pp. 1–31.
6 L. C. Bock, L. C. Griffin, J. A. Latham, E. H. Vermaas and J. J. Toole, *Nature*, 1992, **355**, 564–566.
7 L. R. Paborsky, S. N. Mccurdy, L. C. Griffin, J. J. Toole and L. K. Leung, *Thromb. Haemostasis*, 1993, **69**, 889.
8 J. R. Williamson, *Annu. Rev. Biophys. Biomol. Struct.*, 1994, **23**, 703–730.
9 N. Maizels, M. L. Duquette, P. Handa, J. A. Vincent and A. F. Taylor, *Genes Dev.*, 2004, **18**, 1618–1629.
10 C. K. Tison and V. T. Milam, *Soft Matter*, 2010, **6**, 4446–4453.
11 T. Delange, *Proc. Natl. Acad. Sci. U. S. A.*, 1994, **91**, 2882–2885.
12 P. H. Bolton and H. Arthanari, *Chem. Biol.*, 2001, **8**, 221–230.
13 N. J. Jing, R. F. Rando, Y. Pommier and M. E. Hogan, *Biochemistry*, 1997, **36**, 12498–12505.
14 L. H. Hurley, A. Siddiqui-Jain, C. L. Grand and D. J. Bearss, *Proc. Natl. Acad. Sci. U. S. A.*, 2002, **99**, 11593–11598.
15 D. Y. Sun, A. Pourpak, K. Beetz and L. H. Hurley, *Clin. Cancer Res.*, 2003, **9**, 6122s–6123s.
16 J. C. Soria, K. A. Olaussen, K. Dubrana, J. Dornont, J. P. Spano and L. Sabatier, *Crit. Rev. Oncol. Hematol.*, 2006, **57**, 191–214.
17 N. Sugimoto, D. Miyoshi and A. Nakao, *Nucleic Acids Res.*, 2003, **31**, 1156–1163.
18 D. Sen and W. Gilbert, *Nature*, 1990, **344**, 410–414.
19 A. T. Phan, K. N. Luu, V. Kuryavyi, L. Lacroix and D. J. Patel, *J. Am. Chem. Soc.*, 2006, **128**, 9963–9970.
20 K. R. Fox, P. A. Rachwal and T. Brown, *FEBS Lett.*, 2007, **581**, 1657–1660.
21 S. Balasubramanian and A. Bugaut, *Biochemistry*, 2008, **47**, 689–697.
22 K. R. Fox, P. A. Rachwal and T. Brown, *Biochemistry*, 2007, **46**, 3036–3044.
23 K. Phillips, Z. Dauter, A. I. H. Murchie, D. M. J. Lilley and B. Luisi, *J. Mol. Biol.*, 1997, **273**, 171–182.
24 J. Feigon, N. V. Hud and P. Schultze, *J. Am. Chem. Soc.*, 1998, **120**, 6403–6404.
25 N. V. Hud, P. Schultze, V. Sklenar and J. Feigon, *J. Mol. Biol.*, 1999, **285**, 233–243.
26 F. M. Chen, *Biochemistry*, 1992, **31**, 3769–3776.

27 J. Deng, Y. Xiong and M. Sundaralingam, *Proc. Natl. Acad. Sci. U. S. A.*, 2001, **98**, 13665–13670.
28 L. A. Marky and B. I. Kankia, *J. Am. Chem. Soc.*, 2001, **123**, 10799–10804.
29 A. Wlodarczyk, P. Grzybowski, A. Patkowski and A. Dobek, *J. Phys. Chem. B*, 2005, **109**, 3594–3605.
30 F. W. Kotch, J. C. Fettinger and J. T. Davis, *Org. Lett.*, 2000, **2**, 3277–3280.
31 I. Smirnov and R. H. Shafer, *J. Mol. Biol.*, 2000, **296**, 1–5.
32 P. R. Majhi and R. H. Shafer, *Biopolymers*, 2006, **82**, 558–569.
33 J. L. Mergny, J. Gros, A. De Cian, A. Bourdoncle, F. Rosu, B. Sacca, l. Guittat, S. Amrane, M. Mills and P. Alberti, in *Energetics, Kinetics and Dynamics of Quadruplex Folding*, ed. S. Neidle and S. Balasubramanian, Royal Society of Chemistry, Cambridge, UK, 2006, pp. 31–80.
34 W. Liu, Y. Fu, B. Zheng, S. Cheng, W. Li, T. C. Lau and H. Liang, *J. Phys. Chem. B*, 2011, **115**, 13051–13056.
35 W. Liu, H. Zhu, B. Zheng, S. Cheng, Y. Fu, W. Li, T. C. Lau and H. Liang, *Nucleic Acids Res.*, 2012, **40**, 4229–4236.
36 R. F. Macaya, P. Schultze, F. W. Smith, J. A. Roe and J. Feigon, *Proc. Natl. Acad. Sci. U. S. A.*, 1993, **90**, 3745–3749.
37 N. J. Jing and M. E. Hogan, *J. Biol. Chem.*, 1998, **273**, 34992–34999.
38 N. Sugimoto, T. Toda and T. Ohmichi, *Chem. Commun.*, 1998, 1533–1534.
39 S. L. Forman, J. C. Fettinger, S. Pieraccini, G. Gottareli and J. T. Davis, *J. Am. Chem. Soc.*, 2000, **122**, 4060–4067.
40 Y. Wang and D. J. Patel, *Structure*, 1993, **1**, 263–282.
41 D. M. Gray, S. H. Hung and K. H. Johnson, *Methods Enzymol.*, 1995, **246**, 19–34.
42 E. Hatzakis, K. Okamoto and D. Yang, *Biochemistry*, 2010, **49**, 9152–9160.
43 R. D. Gray and J. B. Chaires, *Nucleic Acids Res.*, 2008, **36**, 4191–4203.
44 J. Plavec and N. V. Hud, in The Role of Cations in Determining Quadruplex Structure and Stability, *Quadruplex Nucleic Acids*, ed. S. Neidle and S. Balasubramanian, Royal Society of Chemistry, Cambridge, UK, 2006, p. 100.
45 B. Pagano, L. Martino, A. Randazzo and C. Giancola, *Biophys. J.*, 2008, **94**, 562–569.
46 P. Podbevsek, N. V. Hud and J. Plavec, *Nucleic Acids Res.*, 2007, **35**, 2554–2563.
47 P. Hazel, J. Huppert, S. Balasubramanian and S. Neidle, *J. Am. Chem. Soc.*, 2004, **126**, 16405–16415.
48 R. V. Reshetnikov, J. Sponer, O. I. Rassokhina, A. M. Kopylov, P. O. Tsvetkov, A. A. Makarov and A. V. Golovin, *Nucleic Acids Res.*, 2011, **39**, 9789–9802.